Available online at www.sciencedirect.com
SCIENCE DIRECT®
Journal of Organometallic Chemistry 664 (2002) 123–129
Journal of Organometallic Chemistry
www.elsevier.com/locate/jorganchem

Synthesis and electrochemical behaviour of σ,η²-acetylide-bridged early–late complexes; The solid-state structure of $[(\eta^5\text{-}C_5H_4SiMe_3)_2Ti(C{\equiv}C\text{-}SiMe_3)_2]Pd(PPh_3)$

Stephan Back [a], Thomas Stein [a], Joachim Kralik [a], Christian Weber [a], Gerd Rheinwald [a], Laszlo Zsolnai [b], Gottfried Huttner [b,1], Heinrich Lang [a,*]

[a] Technische Universität Chemnitz, Institut für Chemie, Fakultät für Naturwissenschaften, Lehrstuhl Anorganische Chemie, Straße der Nationen 62, D-09111 Chemnitz, Germany
[b] Universität Heidelberg, Anorganisch-Chemisches Institut, Im Neuenheimer Feld 270, 69120 Heidelberg, Germany

Received 27 June 2002; accepted 11 September 2002

Abstract

Based on the bis(alkinyl) titanocene $[Ti](C{\equiv}CSiMe_3)_2$ (**1**) a series of mixed early–late metal complexes of the general type $\{[Ti](C{\equiv}CSiMe_3)_2\}ML$ $\{[Ti] = (\eta^5\text{-}C_5H_4SiMe_3)_2Ti$; M = Ni, Pd; L = PPh_3, $P(OMe)_3$, $P(OPh)_3\}$ was prepared. The solid-state structure of $\{[Ti](C{\equiv}CSiMe_3)_2\}Pd(PPh_3)$ (**2**) is reported. Complex **2** exhibits typical features of early–late heterobimetallic tweezer complexes: (i) a pseudo-tetrahedrally coordinated Ti(IV) centre; (ii) a trigonal-planar coordination sphere around the Pd(0) centre, comprised of the two η²-coordinated $Me_3SiC{\equiv}C$ entities and the datively-bound PPh_3 ligand; (iii) a lengthening of the C≡C triple bonds upon their η²-coordination to Pd(0); and (iv) a *trans*-deformation of the Ti–C≡C–$SiMe_3$ units due to the tweezer effect. Cyclic voltammetric studies on **2** and $\{[Ti](C{\equiv}CSiMe_3)_2\}NiL$ [**3**, L = CO; **4a**, L = $P(OCH_3)_3$] reveal an electron donating character of the coordinated M(0) centres, which is demonstrated by the shift of the Ti(IV)/Ti(III) reduction to a more negative potential. This reductive process also exhibits a dependence on the π-acidity of the respective Lewis-base L.

Keywords: π-Tweezer; Cyclic voltammetry; Early–late complex; π-Acidity; Titanium; Palladium; Nickel; Solid-state structure

1. Introduction

The reaction chemistry of bis(alkynyl) titanocenes like $[Ti](C{\equiv}CSiMe_3)_2$ $\{[Ti] = (\eta^5\text{-}C_5H_4SiMe_3)_2Ti\}$ towards various late transition metal (TM) complexes has been investigated thoroughly in the recent years [1]. A wide variety of Ti(IV)-containing early–late mixed metal complexes of general type $\{[Ti](C{\equiv}CR)_2\}ML$ (ML = low-valent TM fragment, R = singly-bound organic ligand) could be synthesised with group 6–12 metal atoms of the periodic table of the elements in different oxidation states [2–6]. Also, alkaline and earth alkaline metals could successfully be introduced in the bis(alkynyl) titanocene framework, however, with titanium in the oxidation state +3 [7]. The solid-state structures of representative examples were reported [1–7]. It could be shown that within these arrangements two TM centres are held in close proximity by a σ,η²-coordination mode of the appropriate titanium-bound acetylides RC≡C. The corresponding complexes $\{[Ti](C{\equiv}CR)_2\}ML$ feature an electron-poor d^0 metal [Ti(IV)] and, e.g. an electron-rich d^{10} metal [such as Cu(I) or Ni(0)], respectively. However, the electronic effects which exerts a bis-η²-coordinated low-valent TM centre complex fragment

* Corresponding author. Tel.: +49-371-5311200; fax: +49-371-5311833
E-mail address: heinrich.lang@chemie.tu-chemnitz.de (H. Lang).
[1] To whom correspondence should be addressed pertaining X-ray structure analysis.

0022-328X/02/$ - see front matter © 2002 Elsevier Science B.V. All rights reserved.
PII: S0022-328X(02)01972-1

with the TM in a low oxidation state, such as Ni(0) or Pd(0), have drawn less attention. Only recently, the electrochemical behaviour of heterotrimetallic bis(alkynyl) titanocenes of type $[Ti][(C\equiv C)_nFc]_2$ ($n = 1, 2$) [8] has attracted much interest due to a novel, oxidatively induced bond cleavage of the $Ti-C_{C\equiv C}$ σ-bonds [8,9], which gives access to bis(ferrocenyl)-butadiyne or -octatetrayne $Fc(C\equiv C)_nFc$ species ($n = 2, 4$) [8,9]. While the tweezer complexes $[Ti][(C\equiv C)_nFc]_2$ ($n = 1, 2$) selectively produce the corresponding $Fc(C\equiv C)_nFc$ species ($n = 2, 4$), it was found that this $Ti-C_{C\equiv C}$ σ-bond cleavage can partly be prevented when the $Ti(C\equiv C)_2$ entities are η^2-coordinated to a copper(I) bromide group as given in $\{[Ti](C\equiv CFc)_2\}CuBr$ [10]. In other cases, a shift of the Ti(IV)/Ti(III) reduction to a more negative potential was observed, depending on the coordinated d^{10}-configurated TM complex fragment [9,11]. The latter finding can be explained by an electron donating effect of the bis-η^2-coordinated TM complex fragment, e.g. $(\eta^2\text{-}C\equiv CR)_2Ni(CO)$ [8c].

In order to determine the electronic influence of an electron-rich TM atom on an electron-deficient TM centre, which is connected via a π-conjugated organic system, a variety of early–late mixed metal complexes of the type $\{[Ti](C\equiv CSiMe_3)_2\}ML$ was prepared [M = Ni, Pd; L = $P(OMe)_3$, $P(OPh)_3$, PPh_3] and studied by cyclic voltammetry.

2. Results and discussion

2.1. Synthesis and characterisation of 2–4

The reaction of $[Ti](C\equiv CSiMe_3)_2$ (**1**) [12] with ML_4 (M = Pd, Ni; L = CO, PPh_3) in a 1:1 molar ratio produces the corresponding heterobimetallic complexes $\{[Ti](C\equiv CSiMe_3)_2\}ML$ [**2**: ML = $Pd(PPh_3)$; **3**: ML = Ni(CO)] [13] by loss of PPh_3 or CO [Reaction (i) and (ii), Scheme 1].

After heating a toluene solution containing **3** and $P(OR)_3$ (R = Me, Ph) to 90 °C (R = Me) or reflux (R = Ph), the nickel-bound CO ligand is replaced by the appropriate $P(OR)_3$ entity. This affords phosphite complexes of the type $\{[Ti](C\equiv CSiMe_3)_2\}Ni[P(OR)_3]$ (**4a**: R = Me, **4b**: R = Ph) [Reaction (iii), Scheme 1] in a very good yield [14].

Since, the spectroscopic and structural data of **4a** and **4b** were reported recently, only heterobimetallic **2** is discussed in detail here. The IR spectrum of **2** exhibits the characteristic C≡C stretching vibration at 1816 cm^{-1} (Table 1). In comparison to complex **1** [12] this absorption is shifted to lower wavenumbers (c.f. **1**: 2012 cm^{-1}).

In contrast, for **4a** and **4b** two stretching vibrations are observed [**4a**: 1807 and 1785 cm^{-1}, **4b**: 1812 and 1788 cm^{-1}] (Table 1) [14], which can best be explained

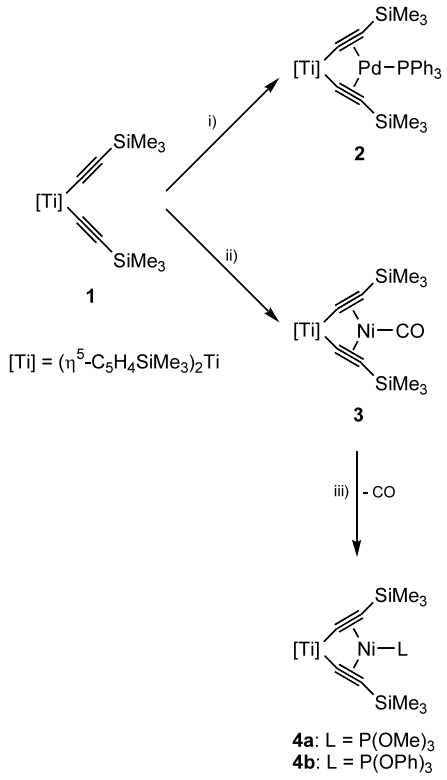

Scheme 1. Reaction of **1** with $Pd(PPh_3)_4$ and $Ni(CO)_4$ to produce **2** and **3** [13]. Synthesis of **4a** and **4b** by treatment of **3** with $P(OR)_3$ (R = CH_3, C_6H_5) [14]. (i) $Pd(PPh_3)_4$, toluene/*n*-pentane, 25 °C; (ii) $Ni(CO)_4$, toluene/*n*-pentane, 25 °C; (iii) $P(OMe)_3$, toluene, 90 °C or $P(OPh)_3$, toluene, reflux.

by a transfer of one acetylenic unit from the bis(alkynyl) titanocene fragment to Ni(0) [14]. Thereby, the nickel atom is formaly oxidised to Ni(I) and the Ti(IV) centre is reduced to Ti(III) (Scheme 2). A similar behaviour of such Ti(IV)–Ni(0) complexes in solution have been made by Rosenthal et al. [15]. A detailed discussion can be found there and in recent reviews [1a,15].

The ^{1}H-NMR spectrum of **2** shows well resolved resonance signals for each of the organic groups present. Compared to the starting compound **1** [12] the characteristic pseudo-triplets of the cyclopentadienyl ligands in **2** are shifted by ca. 1 ppm to higher field, which is typical for this type of tweezer molecules (Table 1).

The $^{13}C\{^1H\}$-NMR spectrum of **2** shows that the C_α signal for **2** ($TiC_\alpha\equiv C_\beta$ is shifted by ca. 35 ppm to lower field (c.f. **1**: 172.5 ppm) [12], while the resonance signal of C_β (113.9 ppm) is shifted to higher field when compared to **1** (135.4 ppm) [12].

The $^{31}P\{^1H\}$-NMR spectrum of **2** exhibits the expected phosphorous resonance signal at 31.3 ppm. A similar chemical shift is also observed, for example, for $\{[Ti](C\equiv CFc)_2\}Pd(PPh_3)$ (36.8 ppm) [9,16].

The EI-MS spectrum of **2** reveals the corresponding molecular ion $[M^+]$ ($m/z = 884$) and the characteristic fragmentation ion $[M^+]$ –$Pd(PPh_3)$ at $m/z = 524$.

Table 1
Most significant spectroscopic data for complex **2** (**1**, **4a** and **4b** for comparison) [12,14]

Compound	IR [a] (cm^{-1})	^{1}H-NMR [b]	$^{13}C\{^1H\}$-NMR [b]		$^{31}P\{^1H\}$-NMR [c] δ (ppm)
		$C_5H_4SiMe_3$ [d] δ (ppm) (J_{HH} (Hz))	$TiC_\alpha{\equiv}C_\beta$ δ (ppm)	$TiC_\alpha{\equiv}C_\beta$ δ (ppm)	
1	2012	6.15 (2.4) 6.66 (2.4)	172.5	135.4	–
2	1816	5.45 (2.1) 5.65 (2.1)	207.3	113.9	31.3
4a	1807, 1785	5.12 (2.2) 5.47 (2.2)	– [e]	123.4	169.5
4b	1812, 1788	5.10 (2.3) 5.47 (2.3)	166.1	– [e]	146.2

[a] Recorded in KBr.
[b] Recorded in $CDCl_3$ with the solvent signal as internal reference (relative to $SiMe_4 = 0.00$ ppm).
[c] Recorded in $CDCl_3$ with $P(OMe)_3$ ($\delta = 139.0$ ppm) as external reference (relative to $H_3PO_4 = 0.00$ ppm).
[d] Appear as pseudo-triplets.
[e] Could not be unequivocally assigned.

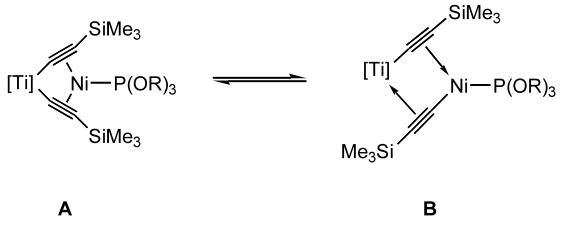

Scheme 2. Structural behaviour of **4a** and **4b** in solution; equilibrium between structural type **A** and **B** molecules.

2.2. Solid-state structure

By cooling a toluene/*n*-pentane solution containing **2** to −30 °C, single red crystals of **2** could be obtained. The solid-state structure of **2** is depicted in Fig. 1. Structural details are listed in Table 2 and the crystal and collection data are summarised in Table 3 (Section 4).

Heterobimetallic **2** crystallises in the triclinic space group $P\bar{1}$. The unit cell contains two independent molecules, which differ only in the positioning of a disordered $C_5H_4SiMe_3$ ligand, and, as a consequence thereof, a disordered $SiMe_3$ residue of one $Me_3SiC{\equiv}C$ group (occupancy factors 0.46192 and 0.53808). However, all other relevant structural properties of the $Ti(C{\equiv}CSiMe_3)PdP$ array remain thereby unaffected. Therefore, only one molecule is depicted in Fig. 1.

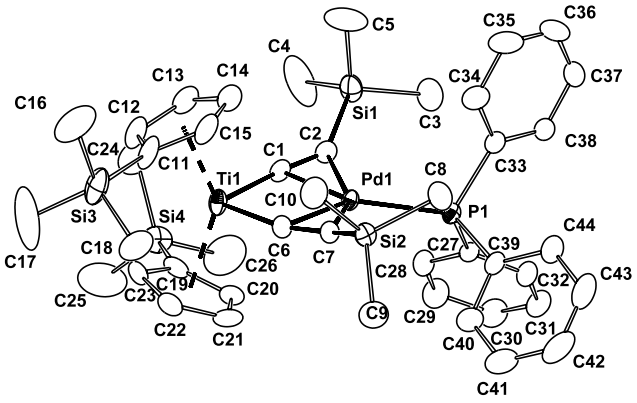

Fig. 1. ZORTEP-plot (30% probability level) of **2** with the molecular geometry and atom numbering scheme. Shown is the molecule with occupancy factor 0.53808.

Table 2
Bond distances (Å) and angles (°) for **2** [a]

Bond distances			
Pd(1)–P(1)	2.3087(13)	Pd(1)–C(1)	2.186(4)
Ti(1)–C(1)	2.087(4)	Pd(1)–C(2)	2.305(4)
Ti(1)–C(6)	2.110(4)	Pd(1)–C(6)	2.189(4)
C(1)–C(2)	1.257(5)	Pd(1)–C(7)	2.285(4)
C(6)–C(7)	1.261(5)	Ti(1)–D(1) [b]	2.088(23)
C(2)–Si(1)	1.832(6)	Ti(1)–D(2) [b]	1.968(12)
C(7)–Si(2)	1.857(4)		
Bond angles			
Ti(1)–Pd(1)–P(1)	168.76(3)	C(1)–C(2)–Si(1)	146.3(3)
Ti(1)–C(1)–C(2)	165.8(3)	C(6)–C(7)–Si(2)	147.4(3)
Ti(1)–C(6)–C(7)	163.9((3)	D(1) [b]–Ti(1)–D(2) [b]	136.36(69)
C(1)–Ti(1)–C(6)	95.13(14)		

[a] The estimated standard deviations of the last significant digits are shown in parantheses.
[b] D(1), D(2): centroids of the cyclopentadienyl ligands.

Compared to the parent complex $[Ti](C{\equiv}CSiMe_3)_2$ (**1**) [$Ti–C_{C\equiv C}$ 2.124(5), 2.103(5) Å] [12] the $Ti–C_{C\equiv C}$ σ-bond lengths in **2** [Ti(1)–C(1) 2.087(4), Ti(1)–C(6) 2.110(4) Å] are somewhat shorter, due to the η^2-coordination to the late TM fragment $Pd(PPh_3)$. The C≡C triple bond distances in **2** [C(1)–C(2), 1.257(5); C(6)–C(7), 1.261(5) Å] are elongated when compared to the respective distances in **1** [1.214(6), 1.203(9) Å] [12]. These elongations resemble the shift of the corresponding C≡C stretching vibrations to lower wavenumbers (see above). This finding indicates that upon η^2-coordination of the $Me_3SiC{\equiv}C$ units in **1** to a TM atom such

Table 3
Crystal and intensity collection data for **2**

Empirical formula	$C_{44}H_{59}PPdSi_4Ti$
Molecular mass	884.54
Temperature (K)	200(2)
Radiation (λ, Å)	0.71073
Crystal system	Triclinic
Space group	$P\bar{1}$
a (Å)	10.960(6)
b (Å)	14.438(7)
c (Å)	16.295(8)
α (°)	89.89(2)
β (°)	74.77(2)
γ (°)	80.52(2)
V (Å^3)	2452(2)
Z	2
ρ_{calc} (g cm^{-3})	1.198
Absorption coefficient (μ, mm^{-1})	0.686
$F(000)$	924
Crystal dimensions (mm)	0.2 × 0.3 × 0.3
Diffractometer model	Siemens-Nicolet Syntex R3m/V
Scan mode	σ-scan
Scan range (°)	$1.89 \le \theta \le 22.01$
Index ranges	$0 \le h \le 11$, $-15 \le k \le 15$, $-16 \le l \le 17$
Total reflections	6393
Unique reflections	6009
Observed reflections [$I \ge 2\sigma(I)$]	5197
R_{int}, S	0.0360, 1.033 [c]
Refined parameters	579
R_1 [a], wR_2 [b] [$I \ge 2\sigma(I)$]	0.0358, 0.0866
R_1 [a], wR_2 [b] (all data)	0.0452, 0.0914
Max/Min peak in final Fourier map (e Å^{-3})	0.640, −0.603

[a] $R_1 = [\Sigma\ (||F_o| - |F_c||)/\Sigma\ |F_o|]$.
[b] $wR_2 = [\Sigma\ (w(F_o^2 - F_c^2)^2)/\Sigma\ (wF_o^4)]^{1/2}$; $w = 1/[\sigma^2(F_o^2) + (0.0447P)^2 + 1.6125P]$. $P = [F_o^2 + 2F_c^2]/3$.
[c] $S = [\Sigma\ w(F_o^2 - F_c^2)^2]/(n-p)^{1/2}$; n = number of reflections, p = parameters used.

as palladium in **2**, a bond weakening of the C_2-acetylide entities takes place, which is typical for the change from *non*-coordinated to η^2-coordinated alkynyl ligands [1,17a]. The Si–$C_{C\equiv C}$ separations Si(1)–C(2), Si(2)–C(7) are in the range of known values for carbon–silicon single bonds [17b]. The metal–phosphorous distance in **2** [Pd(1)–P(1): 2.3087(13) Å] lies in the range of reported values in, for example, tweezer chemistry ({[Ti](C≡CFc)$_2$}Pd(PPh$_3$) [2.3075(13) Å] [9], [Ti](C≡C–C≡CEt)$_2$}Pd(PPh$_3$)) [14,16,18].

The angle Ti(1)–Pd(1)–P(1) clearly deviates with 168.76(3)° from linearity. Consequently, the phosphorous atom P(1) is located [by 0.6483(33) Å] out of a best plane through the atoms Ti(1)–C(1)–C(6)–C(2)–C(7)–Pd(1) [maximum deviation out of this plane: Pd(1), 13.55(17) Å]. The angles for Ti(1)–C(6)–C(2) and C(1)–C(2)–Si(1), respectively, Ti(1)–C(6)–C(7) and C(6)–C(7)–Si(2), exhibit a typical *trans*-deformation, which results in a zigzag-pattern of the coordinating alkynyl units Ti–C≡C–Si in **2** (Table 2). Compared to **1** [102.8(2)°] [12] the angle enclosed by C(1)–Ti(1)–C(6) [95.13(14)°] in **2** is narrowed due to the bis-η^2-coordination of the two alkynyl units present in **1**. However, the D(1)–Ti(1)–D(2) angle [C(1), D(2) = centroids of the cyclopentadienyl ligands] is, when compared with **1**, not effected.

2.3. Electrochemical behaviour of complexes 2–4

Complexes **2**–**4** are comprised of an early TM in a high oxidation state, i.e. Ti(IV), and a late TM in a low oxidation state, i.e. M(0) (M = Ni, Pd). This proximity of an electron-rich component to the Ti(IV) ion could lead to electrochemically detectable changes in its redox behaviour. Therefore, cyclic voltammetric studies were carried out on complexes **1**–**3** and **4a**. Exemplarily, the cyclic voltammograms of **1**, **2** and **3** are presented in Figs. 2–4. The corresponding data for **1**–**3** as well as **4a** are listed in Table 4.

The π-tweezer molecule [Ti](C≡CSiMe$_3$)$_2$ (**1**) exhibits in tetrahydrofuran as solvent a reversible one-electron reduction at $E_0 = -1.84$ V ($\Delta E = 130$ mV) (Table 4). On introduction of a M(0) atom (M = Ni, Pd) this reduction potential is shifted to a more negative value (−2.4 to −2.8 V) (Table 4). However, in the case of the Ti(IV)–Pd(0) complex **2** an irreversible process is observed at $E_{red} = -2.79$ V, which is followed by the development of a reversible one-electron process at $E_0 = -1.97$ V ($\Delta E = 90$ mV). This can be explained by a reductively initiated loss of the Pd(PPh$_3$) fragment and the reformation of [Ti](C≡CSiMe$_3$)$_2$ (**1**) [9]. A similar observation was made in the case of tetrametallic {[Ti]-(C≡CFc)$_2$}Pd(PPh$_3$) [Fc = (η^5-C$_5$H$_4$)Fe(η^5-C$_5$H$_5$)] [9].

The Ti(IV)–Ni(0) complexes {[Ti](C≡CSiMe$_3$)$_2$}NiL [**3**: L = CO, **4a**: L = P(OMe)$_3$] exhibit a somewhat different behaviour. The reversible one-electron reduction for **3** is observed at $E_0 = -2.48$ V ($\Delta E = 150$ mV),

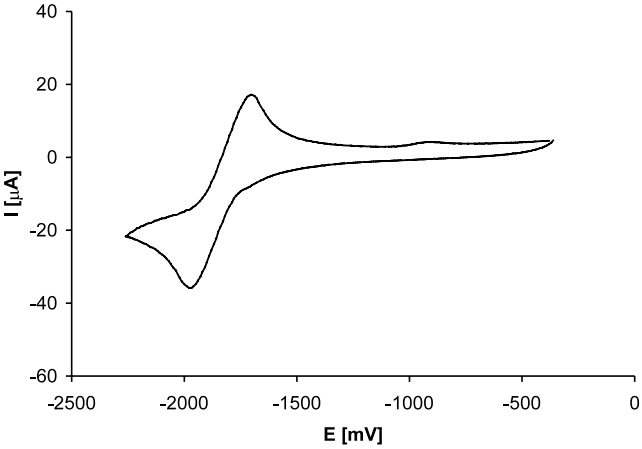

Fig. 2. Cyclic voltammogram of [Ti](C≡CSiMe$_3$)$_2$ (**1**); in a tetrahydrofuran solution in the presence of [*n*-Bu$_4$N][PF$_6$] (c = 0.1 M) at 25 °C under N$_2$; scan rate 100 mV s^{-1}; potentials are referenced to the FcH/FcH$^+$ couple as internal standard.

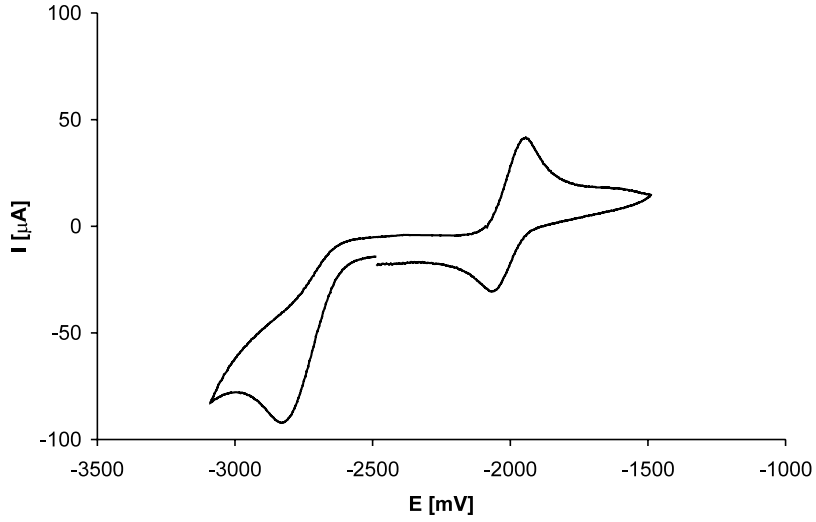

Fig. 3. Cyclic voltammogram of {[Ti](C≡CSiMe$_3$)$_2$}Pd(PPh$_3$) (**2**); in a tetrahydrofuran solution in the presence of [*n*-Bu$_4$N][PF$_6$] ($c = 0.1$ M) at 25 °C under N$_2$; scan rate 100 mV s^{-1}; potentials are referenced to the FcH/FcH$^+$ couple as internal standard.

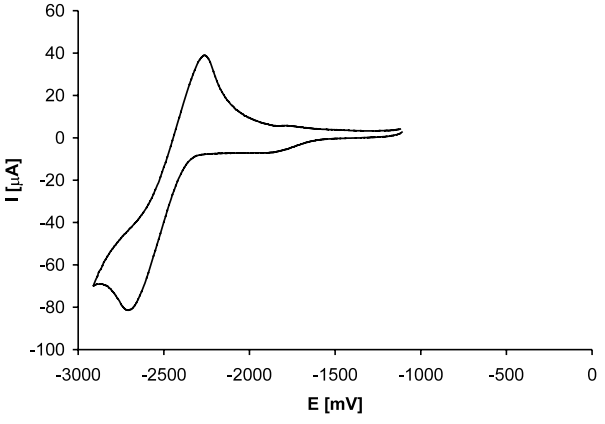

Fig. 4. Cyclic voltammogram of {[Ti](C≡CSiMe$_3$)$_2$}Ni(CO) (**3**) [13]; in a tetrahydrofuran solution in the presence of [*n*-Bu$_4$N][PF$_6$] ($c = 0.1$ M) at 25 °C under N$_2$; scan rate 100 mV s^{-1}; potentials are referenced to the FcH/FcH$^+$ couple as internal standard.

Table 4
Cyclic voltammetric data for **1**–**3** and **4a** [a]

Compound	Reduction	
	E_0 (V)	ΔE (mV)
1	−1.84	130
2	−2.79 [b]	– [b]
3	−2.48	150
4a	−2.71	120

[a] The cyclic voltammograms have been recorded in tetrahydrofuran solutions in the presence of [*n*-Bu$_4$N][PF$_6$] ($c = 0.1$ M) at 25 °C under N$_2$; scan-rate 100 mV s^{-1}; potentials are referenced to the FcH/FcH$^+$ couple.

[b] Irreversible reductive process followed by a reversible wave at $E_0 = -1.97$ V ($\Delta E = 90$ mV).

while **4a** exhibits a reversible one-electron reduction at an even more negative potential, i.e. at $E_0 = -2.71$ V ($\Delta E = 120$ mV) (Table 4). This difference can be explained by the strength of the π-acidity of the Ni-centred ligands L in **3** or **4a**, respectively. While the electron-withdrawing effects of a strong π-acid such as CO results in a smaller shift of the reduction potential, the presence of a weaker π-acid, i.e. P(OMe)$_3$, allows for a larger shift of the corresponding potential of the Ti(IV)/Ti(III) redox process. Although a equilibrium exists between the two forms {[Ti]C≡CSiMe$_3$)$_2$}-Ni[P(OR)$_3$] (Scheme 2, structural type **A** molecule) and {[Ti](C≡CSiMe$_3$)}Ni[P(OR)$_3$](C≡CSiMe$_3$) (Scheme 2, structural type **B** molecule), a reductive process is only observable for the Ti(IV)–Ni(0) type **A** molecule of complex **4a** [11].

3. Conclusions

A series of related early–late TM complexes of the type {[Ti](C≡CSiMe$_3$)$_2$}ML [M = Ni, Pd; L = CO, P(OMe)$_3$, P(OPh)$_3$, PPh$_3$] could be synthesised 1a[13,14]. These species feature an early TM in the oxidation state +IV (Ti) and a late TM in the oxidation state ±0 (Ni, Pd). The solid-state structure of {[Ti]-(C≡CSiMe$_3$)$_2$}Pd(PPh$_3$) (**2**) demonstrates that the late TM is tri-coordinated and possesses a trigonal-planar environment, caused by the η^2-coordinated Me$_3$SiC≡C ligands and the corresponding two-electron donor group PPh$_3$. Cyclic voltammetric studies reveal that the Ti(IV)/Ti(III) redox potential is shifted to a more negative value upon introduction of an electron-rich component. The magnitude of this shift shows a dependence on the π-acidity strength of the ligands L, which means that the introduction of an electron-rich entity leads to a electrochemically detectable influence on the reductive behaviour of the Ti(IV) centre.

4. Experimental

4.1. General methods

All reactions were carried out under an atmosphere of purified nitrogen (O_2 traces: CuO catalyst, BASF AG, Ludwigshafen; H_2O: molecular sieve 4 Å, Riedel de Haën) using standard Schlenk techniques. Tetrahydrofuran and Et_2O were purified by distillation from sodium–benzophenone ketyl; n-C_5H_{12} was purified by distillation from CaH_2. IR spectra were recorded on a Perkin–Elmer 983G or a Perkin–Elmer FT-IR Spectrum 1000 spectrometer. ^{1}H-NMR were recorded on a Bruker Avance 250 spectrometer operating at 250.130 MHz in the Fourier transform mode; $^{13}C\{^1H\}$-NMR spectra were recorded at 62.895 MHz. Chemical shifts are reported in δ units (parts per million) downfield from Me_4Si with the solvent as the reference signal ($CDCl_3$: ^{1}H-NMR $\delta = 7.27$; $^{13}C\{^1H\}$-NMR $\delta = 77.0$). $^{31}P\{^1H\}$-NMR were recorded at 101.255 MHz in $CDCl_3$ with $P(OMe)_3$ as external standard ($\delta = 139.0$, relative to 85% H_3PO_4 ($\delta = 0.00$ ppm)). The EI-MS spectrum was recorded on a Finnigan 8400 mass spectrometer operating in the positive-ion mode. M.p. were determined on a Gallenkamp MFB 595 010 M m.p. apparatus. Microanalysis were performed by the Organisch-Chemisches Institut der Universität Heidelberg. Electrochemical measurements were performed by cyclic voltammetry in THF solutions of [n-Bu_4N][PF_6] (0.1 M) at 25 °C, using a standard three-electrode cell on a Radiometer DEA 101 Electrochemical Analyser. All potentials were referenced to the ferrocene/ferrocenium couple (FcH/FcH^+) as internal standard.

4.2. General remarks

Complexes **1** [12], **3** [13], **4a** and **4b** [1,13–15] were prepared by published procedures. All other chemicals were purchased by commercial providers and used as received.

4.2.1. Synthesis of {[Ti](C≡CSiMe$_3$)$_2$}Pd(PPh$_3$) (2)

Compound **1** (300 mg, 0.58 mmol) and $Pd(PPh_3)_4$ (620 mg, 0.58 mmol) was dissolved in 20 ml of $C_6H_5CH_3$ at 25 °C. After 2 h of stirring at this temperature, all volatiles were removed in oil-pump vacuo. The resulting residue was dissolved in 5 ml of Et_2O and layered with 20 ml of n-C_5H_{12}. After 24 h all PPh_3 has crystallised. The supernatant solution was decanted, concentrated to 5 ml and crystallised at −30 °C. Complex **2** (330 mg, 0.39 mmol, 93% based on **1**) could be obtained as red needles.

M.p.: 151 °C. IR (KBr, cm^{-1}): 1816 (m) [$\nu_{C\equiv C}$]. ^{1}H-NMR ($CDCl_3$): δ −0.25 (s, 18 H, SiMe_3), 0.34 (s, 18H, SiMe_3), 5.45 (pt, $J_{HH} = 2.1$ Hz, 4H, C_5H_4), 5.65 (pt, $J_{HH} = 2.1$ Hz, 4H, C_5H_4), 7.2–7.6 (m, 15 H, C_6H_5). $^{13}C\{^1H\}$-NMR ($CDCl_3$): δ 0.5 (SiMe_3), 1.5 (SiMe_3), 107.4 (CH/C_5H_4), 110.4 ($^iC/C_5H_4$), 115.5 (CH/C_5H_4), 113.9 (d, $^2J_{CP} = 10.1$ Hz, TiC≡C), 128.0 (d, $J_{CP} = 9.3$ Hz, CH/C_6H_5), 129.1 (CH/C_6H_5), 132.1 (d, $J_{CP} = 11.3$ Hz, $^iC/C_6H_5$), 134.8 (d, $J_{CP} = 15.0$ Hz, CH/C_6H_5), 207.3 (TiC≡C). $^{31}P\{^1H\}$-NMR ($CDCl_3$): δ 31.3 (PPh_3). EI-MS [m/z (relative intensity)]: 884 (30) $[M]^+$, 524 (100) $[M-Pd(PPh_3)]^+$. Anal. Calc. for $C_{44}H_{59}PPdSi_4Ti$ (885.57): C, 59.68; H, 6.72. Found: C, 59.90; H, 6.63%.

4.2.2. X-ray structure determination

The solid-state structure of the title compound was determined from single crystal X-ray diffraction. Data collections were performed on a Siemens-Nicolet Syntex R3m/V diffractometer using Mo–K_α radiation. Crystallographic data of **2** are given in Table 3. The structure was solved by direct methods (G.M. Sheldrick, SHELX-97, University of Göttingen, Göttingen, Germany, 1997). An empirical absorption correction was applied. The structure was refined by the least-squares method based on F^2 with all reflections. All *non*-hydrogen atoms were refined anisotropicaly; the hydrogen atoms were placed in calculated positions. The pictures were drawn using ZORTEP (L. Zsolnai, G. Huttner, Heidelberg University, 1994).

5. Supplementary material

Crystallographic data for the structural analysis have been deposited with the Cambridge Crystallographic Data Centre, CCDC no. 188833 for complex **2**. Copies of this information may be obtained free of charge from The Director, CCDC, 12 Union Road, Cambridge CB2 1EZ, U.K. (Fax: +44-1223-336033; e-mail: deposit@ccdc.cam.ac.uk or www: http://www.ccdc.cam.ac.uk).

Acknowledgements

The authors are grateful to the Fonds der Chemischen Industrie and the Deutsche Forschungsgemeinschaft for financial support. T. Jannack is thanked for carrying out the MS measurements. H.L. is grateful to the University of Canterbury for a 'University of Canterbury Erskine Fellowship'.

References

[1] For Reviews in this field see: (a) H. Lang, D.S.A. George, G. Rheinwald, Coord. Chem. Rev. 206–207 (2000) 101;
(b) H. Lang, G. Rheinwald, J. Prakt. Chem./Chemiker Zeitung (1999) 1;
(c) H. Lang, M. Weinmann, Synlett (1996) 1;
(d) J. Manna, K.D. John, M.D. Hopkins, Adv. Organomet. Chem. 38 (1995) 79;

(e) S. Lotz, P.H. van Rooyen, R. Meyer, Adv. Organomet. Chem. 37 (1995) 219;
(f) H. Lang, K. Köhler, S. Blau, Coord. Chem Rev. 143 (1995) 113;
(g) H. Lang, M. Leschke, Heteroatom Chem. 13 (2002) 521;
(h) P.J. Low, M.I. Bruce, Adv. Organomet. Chem. 48 (2002) 71;
(i) R. Choukroun, P. Cassoux, Acc. Chem. Res. 32 (1999) 494;
(j) U. Rosenthal, P.M. Pellny, F.G. Kirchbauer, V.V. Burlakov, Acc. Chem. Res. 33 (2000) 119, Recently published theoretical works in this area;
(k) G. Aullon, S. Alvarez, Organometallics 21 (2002) 2627;
(l) E.D. Jemmis, A.K. Phukan, K.T. Giju, Organometallics 21 (2002) 2254;
(m) A. Kovacs, G. Frenking, Organometallics 18 (1999) 887.

[2] (a) M.D. Janssen, K. Köhler, M. Herres, A. Dedieu, W.J.J. Smeets, A.L. Spek, D.M. Grove, H. Lang, G. van Koten, J. Am. Chem. Soc. 118 (1996) 4817;
(b) H. Lang, M. Herres, K. Köhler, S. Blau, S. Weinmann, M. Weinmann, G. Rheinwald, W. Imhof, J. Organomet. Chem. 505 (1993) 85.

[3] W. Frosch, S. Back, K. Köhler, H. Lang, J. Organomet. Chem. 601 (2000) 226.

[4] (a) H. Lang, K. Köhler, L. Zsolnai, M. Büchner, A. Driess, G. Huttner, J. Strähle, Organometallics 18 (1999) 598;
(b) H. Lang, M. Herres, L. Zsolnai, Organometallics 12 (1993) 5008.

[5] K. Köhler, S.J. Silverio, I. Hyla-Kryspin, R. Gleiter, L. Zsolnai, A. Driess, G. Huttner, H. Lang, Organometallics 16 (1997) 4970.

[6] (a) K. Yasafuku, M. Yamazaki, Bull. Chem. Soc. Jpn. 45 (1972) 2664;
(b) H. Lang, S. Blau, B. Nuber, L. Zsolnai, Organometallics 14 (1995) 3216;
(c) N. Mansilla, G. Rheinwald, H. Lang, J. Organomet. Chem. 602 (2000) 72.

[7] (a) V. Varga, J. Hiller, M. Polasek, U. Thewalt, K. Mach, J. Organomet. Chem. 514 (1996) 219;
(b) V. Varga, J. Hiller, U. Thewalt, M. Polasek, K. Mach, J. Organomet. Chem. 553 (1998) 15.

[8] (a) Y. Hayashi, M. Osawa, K. Kobayashi, Y. Wakatsuki, J. Chem. Soc. Chem. Commun. (1996) 1617;
(b) Y. Hayashi, M. Osawa, Y. Wakatsuki, J. Organomet. Chem. 542 (1997) 241;
(c) S. Back, H. Pritzkow, H. Lang, Organometallics 17 (1998) 41;
(d) For a related Hf(IV)-complex see: S. Back, G. Rheinwald, L. Zsolnai, G. Huttner, H. Lang, J. Organomet. Chem. 563 (1999) 73.

[9] S. Back, G. Rheinwald, H. Lang, Organometallics 18 (1999) 4119.

[10] S. Back, G. Rheinwald, H. Lang, J. Organomet. Chem. 601 (2000) 93.

[11] S. Back, W. Frosch, T. Stein, G. Rheinwald, H. Lang, Inorg. Chim. Acta, in print.

[12] (a) H. Lang, M. Herres, L. Zsolnai, Organometallics 12 (1993) 5008;
For related complexes see also: (b) G.L. Wood, C.B. Knobler, M.F. Hawthorne, Inorg. Chem. 28 (1989) 382;
(c) A. Sebald, P. Fritz, B. Wrackmeyer, Spectrochim. Acta 41A (1985) 1405;
(d) R. Jimenez, M.C. Barral, V. Moreno, A. Santos, J. Organomet. Chem. 174 (1979) 281;
(e) A.D. Jenkins, M.F. Lappert, R.C. Srivastava, J. Organomet. Chem. 23 (1970) 165;
(f) J.H. Teuben, H.J. Liefde Meijer, J. Organomet. Chem. 17 (1969) 87;
(g) M. Köpf, M. Schmidt, J. Organomet. Chem. 10 (1967) 383.

[13] H. Lang, M. Herres, L. Zsolnai, W. Imhof, J. Organomet. Chem. 409 (1991) C7.

[14] H. Lang, E. Meichel, Th. Stein, Ch. Weber, J. Kralik, G. Rheinwald, J. Organomet. Chem. 664 (2002) 150.

[15] U. Rosenthal, S. Pulst, P. Arndt, A. Ohff, A. Tillack, W. Baumann, R. Kempe, V.V. Burlakov, Organometalics 14 (1995) 2961.

[16] (a) J. Kralik, Diploma Thesis, Heidelberg University, 1995;
For reviews on Ni-phosphine and -phosphite complexes see also:
(b) L. Sacconi, F. Mani, A. Bencini, in: G. Wilkinson, R.D. Gillard, J.A. McCleverty (Eds.), Compr. Coord. Chem., vol. 5, Pergamon Press, 1987, p. 1;
(c) P.W. Jolly, Compr. Organomet. Chem. 6 (1983) 15.

[17] (a) J. Dale, Properties of acetylenic compounds, in: H.G. Viehe (Ed.), Chemistry of the Acetylenes, Dekker, New York, 1969;
(b) J.Y. Corey, in: S. Patai, Z. Rappoport (Eds.), The Chemistry of Organic Silicon Compounds, Wiley Interscience, 1989.

[18] (a) M. Ciriano, J.A. Howard, J.L. Spencer, F.G.A. Stone, H. Wadepohl, J. Chem. Soc. Dalton Trans. (1979) 1749;
(b) H. Lang, I.Y. Wu, S. Weinmann, C. Weber, B. Nuber, J. Organomet. Chem. 541 (1997) 157.